Supplementary Material for:

Development and laboratory evaluation of a do-it-yourself (DIY) filtration solution for residential evaporative coolers to reduce indoor wildfire smoke exposure

Aditya Singh[1], Brent Stephens[1]*, Mohammad Heidarinejad[1], Brett Stinson[2], Elliott Gall[2], Jeff Wagner[3], Brett Singer[4], Shelly Miller[5], Nayamin Martinez[6], Ruben Rodriguez[6], Gina Solomon[7,8]

[1] Department of Civil, Architectural, and Environmental Engineering, Illinois Institute of Technology, Chicago, IL USA
[2] Department of Mechanical and Materials Engineering, Portland State University, Portland, OR USA
[3] California Department of Public Health, Environmental Health Laboratory Branch, Richmond, CA USA
[4] Lawrence Berkley National Laboratory, Berkeley, CA USA
[5] University of Colorado, Boulder, CO USA
[6] Central California Environmental Justice Network, Fresno, CA USA
[7] Public Health Institute, Oakland, CA USA
[8] School of Medicine, University of California, San Francisco, CA USA

*Corresponding author:
Brent Stephens, PhD
Professor and Department Chair
Arthur W. Hill Endowed Chair in Sustainability
Department of Civil, Architectural, and Environmental Engineering
Illinois Institute of Technology
Alumni Memorial Hall Room 228
3201 S Dearborn Street
Chicago, IL 60616 USA

Figure S1. Three horizontal-flow (through-the-window/wall) residential ECs acquired for laboratory testing: a-c) Essick RN35W, d-f) Phoenix/Brisa BW4002, and g-i) MasterCool MCP44.

Laboratory Measurements of EC Performance

Airflow Rates. An Extech AN200 vane anemometer was used to measure the air velocity leaving the EC supply at 12 points following a grid pattern at the supply grille. Air velocity measurements were made with the anemometer approximately 2.5 cm (1 inch) from the face of the supply grille. The edge points of the grid pattern were at least 4 cm (1.5 inches) away from each edge of the supply grille. After recording the velocity at the 12 points, an average velocity was calculated, which was then multiplied by the measured supply grille gross area to estimate the airflow rate. The uncertainty in airflow rate measurements was estimated using manufacturer-reported uncertainty for velocity measurements, which is ± (3% of reading + 0.2 m/s). We did not propagate uncertainty for repeated velocity measurements, nor did we estimate the uncertainty in the supply grille cross sectional area; the former is not customarily done with such repeated measurements with the same instrument and uncertainty in dimension measurements is challenging to accurately quantify. The anemometers were purchased new and thus were recently factory calibrated. Repeatability in airflow rate measurements were investigated by having at least two researchers periodically repeat velocity traverse measurements at the same test conditions. Three randomly selected test conditions were initially used to make repeated airflow rate measurements by two different researchers, which resulted in a mean difference of less than 2% between the researchers, confirming that airflow rate measurements were repeatable.

Power Draw. Uncertainty in power draw measurements was taken as that reported by the instrument manufacturer (±0.2% of reading). The power draw meters were purchased new and thus recently factory calibrated. Repeatability for this measure was observed as high by visual inspection of data at the same conditions.

Pressure Drop. Uncertainty in pressure drop measurements was taken was that reported by the instrument manufacturer (±1% of reading). The DG-700s are approximately 10 years old but were sent to the manufacturer for calibration in 2022. Repeatability for this measure was noted as moderate by visual inspection of data at the same conditions, as the tight configuration and turbulence influenced by the close proximity of the EC fan, pad, and enclosure sometimes prohibited consistently reliable readings.

Sensible and Latent Cooling Capacity. The impact of a subset of test conditions and corresponding airflow rates on sensible and latent cooling capacity of the ECs was evaluated by measuring the temperature and relative humidity (RH) with Onset HOBO U12 T/RH data loggers logging at 1-minute intervals, located at three points: 1) in front of the EC air intake (i.e., upstream), 2) after the cooling pad but before the fan (as a middle point measure), and 3) in the supply air stream (i.e., downstream, or outlet). Only the inlet and outlet measurements (points 1 and 3) were used to characterize the temperature and humidity differences across the EC during these tests. Temperature (T) and RH values were used to calculate absolute humidity (W, in units of kg_w/kg_{da}) for evaluating latent cooling capacity, assuming atmospheric pressure at sea level. Upstream and downstream values of temperature (T) and humidity ratio (HR, or W) were averaged over 2 hours of approximately steady-state operational periods at any test condition to generate a mean and standard deviation (SD) in each value (i.e., upstream and downstream T and upstream and downstream W). Mean (SD) values in each were used to calculate differences across the EC, pad, and any filter attachment (i.e., ΔT & ΔW). Values of ΔT and ΔW were also used to calculate sensible, latent, and total cooling capacity following Equation S1.

$$Q_t = Q_s + Q_l = \dot{m}_{da} C_p \Delta T + \dot{m}_{da} h_{fg} \Delta W \quad \text{(S1)}$$

where Q_t = total cooling capacity (W), Q_s = sensible cooling capacity (W), Q_l = latent cooling capacity (W), $\dot{m}_{da}$ = mass flow rate of dry air leaving the EC via the supply (kg_{da}/s), C_p = specific heat capacity of air (J/[kg_{da}K]), ΔT = temperature difference across the EC, taken as $T_{supply} - T_{intake}$ (K), h_{fg} = specific enthalpy of vaporization (kJ/kg_w), and ΔW = humidity ratio difference across the EC, taken as $W_{supply} - W_{intake}$ (kg_w/kg_{da}). For the evaporative cooling process, Q_t should be near zero, Q_s should be negative, and Q_l should be positive.

Uncertainty in temperature and RH was taken as that reported by the instrument manufacturer: ±0.2°C of reading for temperature and ±2.5-5% of reading for RH (depending on the value of RH measured). To capture a larger range in uncertainty than experimental uncertainty alone, propagated uncertainty in ΔT and ΔW was estimated by adding the standard deviations of the mean upstream and downstream T and W readings in quadrature. Repeatability for this measure was noted as high by visual inspection of time-series data (i.e., when steady state conditions were achieved).

Tables S1 and **S2** show results for cooling capacity from measurements of temperature and relative humidity (RH) measured upstream before the EC air intakes and downstream after the EC supply with the EC operating at approximately steady-state wet conditions under four filter configurations for the Brisa and MasterCool, respectively. The Brisa EC (**Table S1**) was tested without a filter (wet pad only), with two deep-bed filters 10-cm (4-inch) filters (Tex-Air MERV 13 and Rensa CA-13), and with one filtration combination that led to excessive reductions in flow (5-cm (2-inch) Tex-Air MERV 13 plus 5-cm (2-inch) Rensa CA-13). The MasterCool EC (**Table S2**) was tested without a filter (wet pad only), with two deep-bed 10-cm (4-inch) filters (Tex-Air MERV 13 and Rensa CA-13), and with a 10-cm (4-inch) Tex-Air MERV 11 as an option that led to a more moderate flow reduction.

Table S1. Mean (SD) temperature (T), relative humidity (RH), and humidity ratio (W) measured before the intake and after the supply on the Brisa EC operating at approximately steady-state conditions with a wet pad under four filter configurations.

Test Condition	**Before Intake**				**After Supply**			**Supply - Intake**	
	Flow (m^3/h)	T (°C)	RH (%)	W (g_w/kg_{da})	T (°C)	RH (%)	HR (g_w/kg_{da})	T (°C)	W (g_w/kg_{da})
No Filter	3037 (240)	20.8 (0.2)	65.1% (1.8%)	10.0 (0.3)	18.4 (0.3)	86.9% (1.0%)	11.5 (0.4)	-2.4 (0.4)	1.5 (0.5)
Tex-Air 4” MERV 13	2812 (233)	21.6 (0.1)	66.4% (1.2%)	10.8 (0.2)	19.1 (0.5)	88.5% (0.2%)	12.2 (0.2)	-2.5 (0.5)	1.5 (0.3)
Rensa 4” CA MERV 13	2656 (228)	22.0 (0.1)	67.1% (0.1%)	11.0 (0.1)	19.5 (0.1)	88.9% (0.4%)	12.6 (0.1)	-2.5 (0.1)	1.6 (0.2)
Tex-Air 2” + Rensa 2” M13 Combo	2573 (226)	21.6 (0.1)	66.1% (0.2%)	10.4 (0.2)	19.0 (0.1)	87.8% (0.5%)	12.0 (0.2)	-2.6 (0.1)	1.6 (0.3)

Results from the Brisa show that regardless of filter attachment and associated airflow rate, the difference in temperature and humidity ratio between the intake and supply air were similar, with a temperature drop of approximately 2.5°C and an increase in humidity ratio (W) of approximately 1.5-1.6 g_w/kg_{da} in the lab environment regardless of test condition. This suggests that delivered cooling capacity is affected only by airflow and not by synergistic or antagonistic effects due to changes in ΔT or ΔW.

Table S2. Mean (SD) temperature (T), relative humidity (RH), and humidity ratio (W) measured before the intake and after the supply on the MasterCool EC operating at approximately steady-state conditions with a wet pad under four filter configurations.

Test Condition		Before Intake			After Supply			Supply - Intake	
	Flow (m^3/h)	T (°C)	RH (%)	W (g_w/kg_{da})	T (°C)	RH (%)	W (g_w/kg_{da})	T (°C)	W (g_w/kg_{da})
No Filter	2900 (258)	25.0 (0.8)	38.3% (4.7%)	7.5 (0.4)	20.4 (0.8)	62.6% (2.6%)	9.3 (0.2)	-4.6 (1.6)	1.9 (0.5)
Tex-Air 4” MERV 11	1862 (219)	23.5 (1.5)	43.5% (5.5%)	7.7 (0.4)	18.3 (0.5)	71.6% (2.1%)	9.3 (0.1)	-5.2 (1.6)	1.6 (0.4)
Tex-Air 4” MERV 13	1862 (219)	27.3 (0.3)	33.0% (0.7%)	7.4 (0.2)	20.1 (0.2)	67.2% (0.4%)	9.8 (0.1)	-7.2 (0.4)	2.4 (0.3)
Rensa 4” CA MERV 13	1458 (204)	26.9 (0.6)	33.0% (0.8%)	7.3 (0.2)	20.0 (0.5)	67.4% (0.9%)	9.8 (0.2)	-6.9 (0.8)	2.6 (0.2)

Results for the MasterCool were not as clear and were likely affected by higher variability in environmental conditions upstream of the air intakes but did not suggest systematic impacts of airflow rates on ΔT or ΔW. For example, while the Tex-Air 10 cm (4-inch) MERV 11 and MERV 13 filters were measured to have approximately the same airflow rate, ΔT was 2°C higher and ΔW was nearly 1 g_w/kg_{da} higher with the MERV 13, not because of airflow but likely because of a higher entering temperature when the MERV 13 was tested (the air entering the ECs in these tests was surrounding lab air and thus temperature was not precisely controlled). If any relationship can be ascertained, it is that the measurements conducted with filtration attachments that decreased flow rates demonstrated slightly larger ΔT and ΔW than no filter conditions.

Particle Removal Efficiency. Two sets of paired OPCs were used for efficiency testing in the laboratory including one pair during 2022 (prior to summer 2022 pilot testing in the field) and another pair after pilot testing and before full deployment in summer 2023 (two different OPC pairs were used because one OPC was damaged while in the field in 2022). Prior to each round of laboratory testing, the two paired OPCs were calibrated against each other using co-location tests in which both devices were placed in the same location for a period of time (ranging from about 30 to 90 minutes, logging at 1-minute intervals) to measure the same ambient indoor aerosol sample, and a linear regression between the two devices was used to generate co-location calibration factors for each size bin (**Table S3**). Only co-location factors with R^2 above 0.85 were used; factors with R^2 below 0.85, which were present for the two largest size bins in the second round of testing due to very low number concentrations, were excluded and only raw concentration measurements were used for those size bins.

Table S3. Co-location factors for paired MetOne OPCs used in laboratory filtration efficiency measurements.

	Prior to Summer 2022		**After Summer 2022**	
Bin size (µm)	Slope	R^2	Slope	R^2
0.3-0.5	0.875	0.94	0.803	0.99
0.5-1	1.022	0.98	0.856	0.99
1-2.5	0.838	0.97	0.921	0.97
2.5-5	0.887	0.95	0.949	0.91
5-10	1.228	0.96	0.739	0.65
10+	1.233	0.86	0.382	0.21

VOC Removal Efficiency. Sample air was introduced to the PTR-ToF-MS drift tube at 250 mL/min via a 9 m long section of 0.64 cm o.d. PFA tubing heated to 60 °C. The PTR-ToF-MS scanned across 17–490 amu for compounds with proton affinity higher than that of H2O using H3O+ as the primary reagent ion. The operating conditions were as follows: Tdrift = 60 °C, Pdrift = 2.20 mbar, and Udrift = 600 V, which resulted in electric field strength to number density ratio E/N = 135 Td (Townsend, 1 Td = 10-17 V.cm^2). Signal intensities of NO+ (m/z = 29.9970), O2+ (m/z = 31.9892), and the water cluster (H2O)H3O+ (m/z = 37.0289) were respectively about 0.2%, 2%, and 2.5% of the H318O+ (m/z =21.0221) one. The mass axis was calibrated using a hydronium isotope, H318O+ (m/z = 21.0221), NO+ (m/z = 29.9970), and a C6H4I2 fragment (m/z = 203.944), which is an internal standard continuously injected into the drift tube via a heated permeation device (PerMaScal, Ionicon Analytik GmbH, Innsbruck, Austria). Mass spectra were stored in ten-second intervals. Mass spectra were analyzed using PTRViewer 4.0, with VOC peaks elevated due to wildfire smoke identified and corrected for isotopic interferences and quantified using calibration factors determined from a calibration standard that contained BTEX compounds (Apel-Reimer, USA).

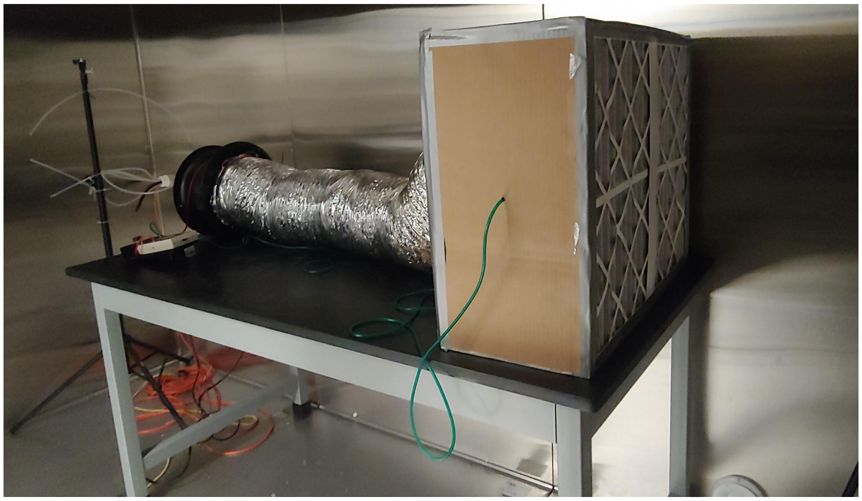

Figure S2. Chamber test setup for measuring VOC removal efficiency of a new 10 cm (4 inch) depth carbon-impregnated MERV 13 filter at Portland State University.

Chamber background concentrations for benzene and toluene were identified visually either before or after decay periods after a short period of approximately steady-state operation. Linear regressions on the natural log transformed concentration data versus time were used to estimate first order loss rate constants during each of the four test conditions, using Equation S2.

$$-ln\left(\frac{C_{i,in}(t) - C_{i,in,bg}}{C_{i,in}(0) - C_{i,in,bg}}\right) = L_i t \quad \text{(S2)}$$

where $C_{i,in}(t)$ = the concentration of constituent *i* at time *t* (ppb), $C_{i,in}(0)$ = the concentration of constituent *i* at time *0* (ppb), $C_{i,in,bg}$ = the steady-state concentration of constituent *i* at a given test condition (ppb), L_i = first order loss rate constant for constituent *i* (1/min), and t = time since the beginning of constituent decay (min). The CADR for constituent *i* at each of the three tested face velocities was then estimated using Equation S3.

$$CADR_i = V(L_{i,test} - L_{i,no\ filter}) \quad \text{(S3)}$$

where $L_{i,test}$ and $L_{i,no\ filter}$ = the estimated first order loss rate constants for constituent *i* in the chamber during a given test condition and without the fan/filter combination operating, respectively, V = the interior volume of the test chamber (17.8 m^3), and $CADR_i$ = the CADR for constituent *i* at the test condition (m^3/min). Finally, the single-pass VOC removal efficiency for constituent *i* was estimated using Equation S4.

$$\eta_i = \frac{CADR_i}{Q_{filter}} \times 100\% \quad \text{(S4)}$$

where η_i = is the estimated single-pass removal efficiency of the filter for constituent *i* at a given test condition (-) and Q_{filter} = the measured flow rate through the filter at a given test condition (m^3/min).

Figure S3 shows an example of time-resolved benzene concentrations measured by the PTR-ToF-MS during chamber testing of a 61x76-cm [24x30-inch] 10-cm [4-inch] depth Rensa CA-13 carbon-impregnated MERV 13 filter and fan combination at Portland State University. The first half of the figure shows benzene elevation (by burning pine needles) followed by natural decay in the enclosed chamber without the fan/filter combination operating, followed by a flush with ambient room air surrounding the chamber. The second half of the figure shows three replicate elevation and decay periods using the same source but with the fan/filter combination operating. The PTR-ToF-MS device switches between chamber and room conditions at the end of each test and the chamber is flushed with room air in between tests. Chamber background (BG) concentrations are selected by visual observation, including BG chamber measurements just before pollutant elevation during the period with the fan/filter switched off ('air cleaner off') and BG chamber measurements at the last few minutes of each decay period with the fan/filter operating ('air cleaner on').

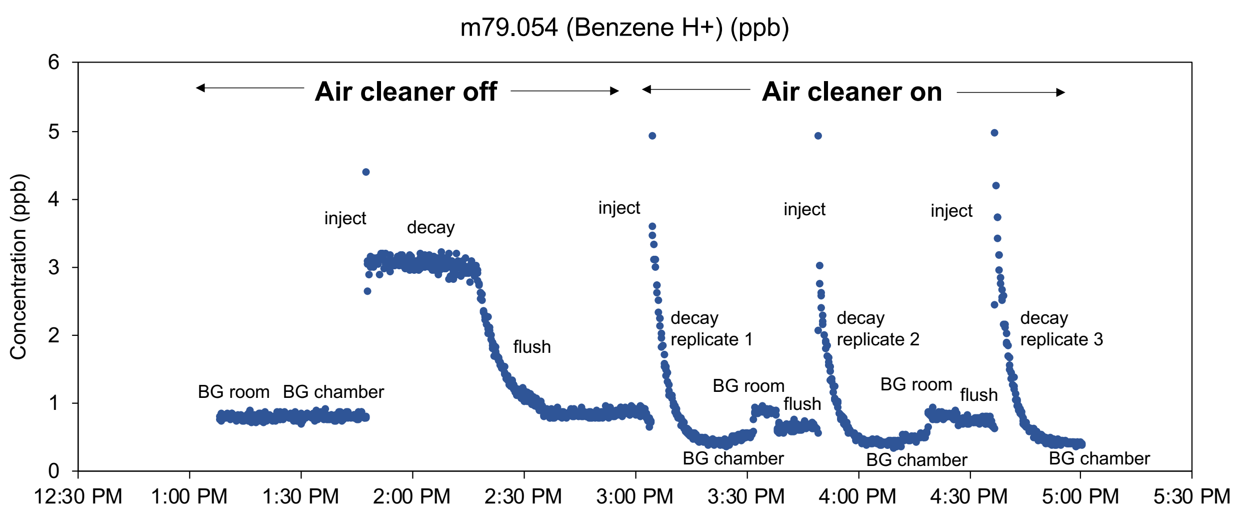

Figure S3. Example of benzene concentrations measured by PTR-ToF-MS during chamber testing of Rensa CA-13 carbon-impregnated MERV 13 filter and fan combination at Portland State University. BG room = background in room outside of chamber, BG chamber = background.

Wildfire Event in Chicago, IL. On two days with heavy wildfire smoke in Chicago, one of the test ECs (Brisa BW4002) was rapidly deployed just outside a set of exterior doors of their laboratory building on campus and fabricated a sheath to mimic a through-the-wall installation of an EC (**Figure S4**).

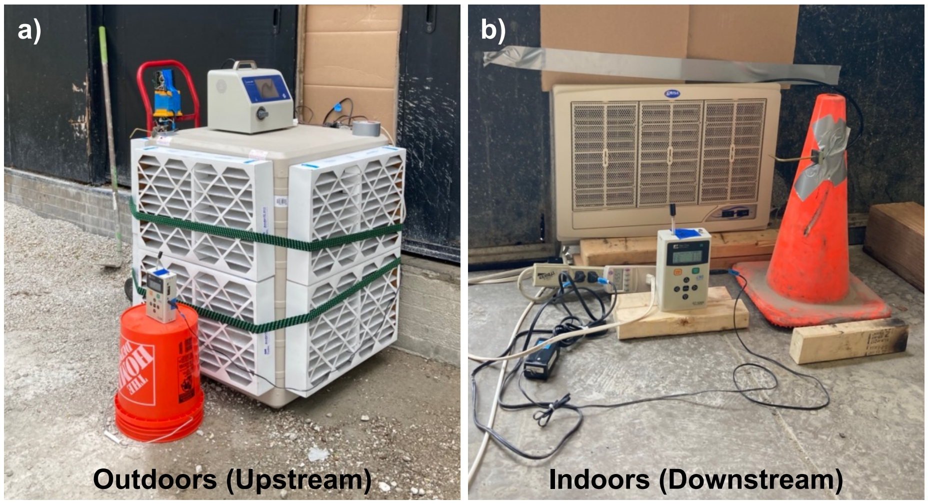

Figure S4. Brisa BW4002 EC and particle monitors (SMPS and two OPCs) deployed outside IIT's laboratory to conduct measurements during the heavy smoke conditions caused by long-range transport from Canadian wildfires to Chicago on June 26-27, 2023: (a) outdoors (upstream) and (b) indoors (downstream).

Testing a plenum structure to house filters

Figure S5 shows results from testing a custom surrounding structure that could act as a plenum and filter housing and allow for filter(s) to be offset from the ECs, potentially reducing moisture issues and leading to longer filter lifespans. A surrounding structure was constructed out of cardboard on just the Brisa unit, allowing for installation of filters on any of the three intake sides. This allowed for evaluating not only the impact of the filters installed in the surrounding structure on performance metrics, but also for evaluating different combinations of filters with varying levels of blockages to better understand the minimum number of filters through which ECs could draw airflow through and still achieve flow performance targets. Therefore, this solution was tested under four conditions, including: (1) three structure openings completely open (mimicking 0% blockage but with the structure in place), (2) filter installed on one intake opening with the other two intakes blocked, (3) filters installed on two intake openings with the other blocked, and (4) filters installed on all 3 intake sides of the structure. These configurations were also chosen for their potential to reduce filter costs, i.e., if only one or two filters could be installed in a larger structure but still maintain flow and efficiency goals, then the upfront filter cost could be reduced. Only the 10-cm (4-inch) Rensa CA-13 filter was tested for these purposes. The structure is shown visually in **Figure S5**a-c. **Figure S5**d shows results from airflow rate testing at these four conditions overlaid on the original Brisa fan curve that was regenerated by progressive blocking and **Figure S5**e shows size-resolved removal efficiency measured across the EC under these test conditions.

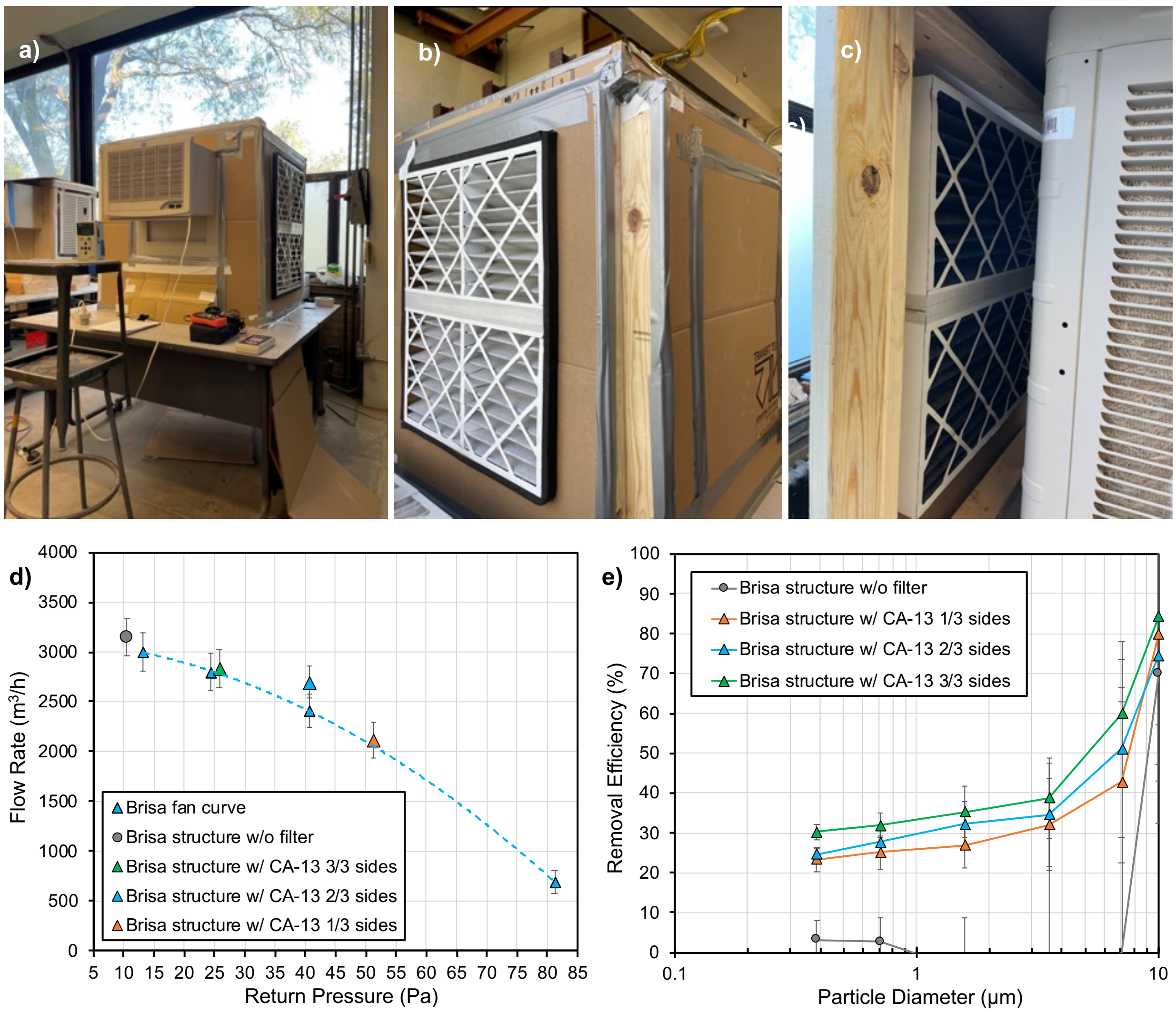

Figure S5. Test results from a custom surrounding structure that could act as a plenum and filter housing and allow for filter(s) to be offset from the ECs: a-c) photos, d) airflow versus pressure drop, e) size-resolved particle removal efficiency.